ACS Macro Letters

Letter

pubs.acs.org/macroletters

Influence of Grafting Surface Curvature on Chain Polydispersity and Molecular Weight in Concave Surface-Initiated Polymerization

Hong Liu,[†] You-Liang Zhu,[†] Jing Zhang,[†] Zhong-Yuan Lu,*[,†] and Zhao-Yan Sun*[,‡]

[†]Institute of Theoretical Chemistry, State Key Laboratory of Theoretical and Computational Chemistry, Jilin University, Changchun 130023, China

[‡]State Key Laboratory of Polymer Physics and Chemistry, Changchun Institute of Applied Chemistry, Chinese Academy of Sciences, Changchun 130022, China

Supporting Information

ABSTRACT: We study living polymerization initiated from concave surfaces. We clarify that, depending on different criteria for ceasing the reaction, different relationships between grafted chain polydispersity index and the grafting surface curvature can be categorized. The average molecular weight of the grafted chains monotonically decreases as the grafting surface curvature increases. These results shed light on better control and design of functional porous materials for use in bioimplanting or chemical sensors.

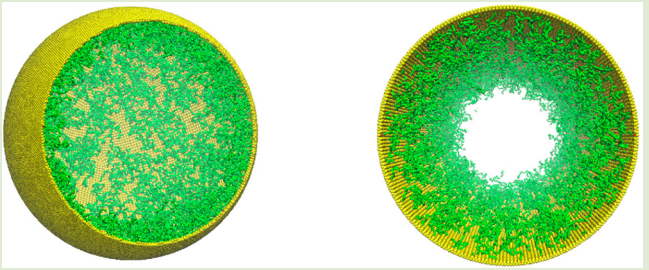

Surface-initiated polymerization (SIP) is one of the most promising polymer-grafting techniques for producing polymer brushes with high grafting density and providing ideal control on polymer architecture and chain length distribution. In many cases, the applications demand the polymer chains to be prepared on different substrate geometries, such as convex, concave, or commonly used flat surfaces. For applications of porous materials in bioimplanting,[1] drug delivery,[2,3] or chemical and biological sensor,[4,5] the modifications of the materials by grafting chains inside concave microcavities or mesopores, such as from inside of porous substrates[6−9] or tube-like channels,[10,11] are becoming more concerned.

Because of the great relevance with the performance of the designed materials, the molecular weight and its distribution, as well as the polydispersity index (PDI) of the grafted chains, are often closely concerned in experiments. Typical methods for determining molecular weight of surface-bound polymers include cleaving the chains from the substrate by chemical treatment and further testing them with a size exclusion chromatograph[12−14] or by gel permeation chromatography.[15] In many situations, these methods are not feasible for insufficiency of cleaved chains from the concave surface. An alternative idea is based on the fact that the molecular weight of the polymer generated in solution from the sacrificial initiator is in good agreement with that of the polymer chains that are cleaved from the surface.[16] Nevertheless, the validity of comparing the results of a solution/bulk polymerization with that of a surface-initiated polymerization is still a matter of debate.[17−19] Due to strong confinement in concave SIP conditions, poor information about molecular weight and PDI has been directly obtained. Genzer and the co-workers speculated[20] on the increase of PDI and decrease of molecular weight in concave SIP, which was supported by experiments.[8,21] Kruk et al.[22] used atom transfer radical polymerization to graft different polymer chains on concave surfaces of cylindrical and spherical mesopores. By appropriately optimizing the grafting process, they obtained very low PDIs and nearly monodisperse chains. Although the above experimental results provide different hints, a general and thorough understanding for the dependence of PDI and molecular weight on grafting surface curvature in concave SIP is still not clear.

The influence of surface curvature on PDI and molecular weight should completely be a physical issue instead of a chemical issue. It may be attributed to the confinement effect on monomer diffusion, or the excluded volume effect on the chain growth space, but should be uncorrelated to the activity of the chain growth centers. In general, for flat-SIP, there are two features hampering the chain growth, that is, the presence of the surface prevents monomer delivery to the active polymer chains from all directions, and the grafting layer formed by the growing polymers may hide a part of the initiators or the chain ends, thus, reducing the effective concentration of monomers near them. Due to reinforced confinement, it is natural to deduce that these two features should be greatly enhanced for concave SIP. Thus, intuitively one may imagine that increasing grafting surface curvature will result in higher PDI for SIP from concave surface. But in this study we show that such dependence is not always true. In our large scale coarse-grained molecular dynamics simulations, we study the SIP inside two types of mesopores, that is, in spherical cavity (Figure 1a) and in cylindrical channel (Figure 1b; we call them

Received: July 3, 2012
Accepted: October 8, 2012
Published: October 10, 2012

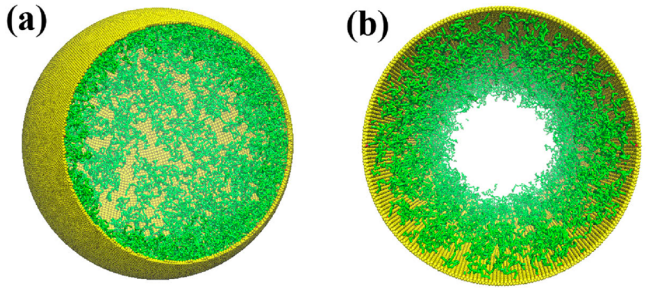

Figure 1. Schematic illustrations of SIP in spherical cavity (a) and in cylindrical channel (b). Yellow beads are frozen to construct the concave grafting surfaces, and green sticks represent grafted polymer chains. The free monomers are omitted for clarity.

as cavity-SIP and channel-SIP in the following). We find that depending on different criteria for *ceasing* the reaction, different relationships between PDI and grafting surface curvature can be categorized.

Our simulation strategies had been described previously.[23] We employ canonical ensemble molecular dynamics simulations combined with stochastic reaction model to design the chain growth process. Matyjaszewki indicated that[24] a well controlled living radical polymerization involves a fast initiation step, negligible chain transfer, and a fast termination. Therefore, most of the computer simulations on living radical SIP were based on the assumption of neglecting initiation and termination processes and chain transfer.[17,18,25] Similarly, to model a true living radical polymerization, we have also neglected these reactions. The concept of reaction probability P_r, which could be considered as the fraction of active chain ends in the total chain ends, is utilized to ensure that we are modeling living polymerization. The fraction of active or dormant chain ends are practically determined by the control agent. The appropriate amount of activator/deactivator is necessary for the controllability of the polymerization,[22] see Supporting Information for detailed explanations. As compared with experiments, the effect from diffusion of the control agent could be simply included in the set of reaction probability. With adopted reaction probability in our simulations, we ensure that the common delivery of free monomers to the active chains is faster than the chain propagation, thus the influence of transport limitation by monomer diffusion to the reaction sites is reasonably negligible.

Pure repulsive truncated-shifted Lennard-Jones (LJ) potential is used to characterize the nonbonded interactions between any two coarse-grained beads for emphasizing the excluded volume effect.[23] Bonded interactions between adjacent monomers in the polymer chain are characterized by a finitely extensible nonlinear elastic spring potential.[23] In our model, the frozen beads are used to construct the concave grafting surfaces. We use the geodesic subdivision method to get all the vertex positions.[26] Then each vertex is occupied by a frozen bead in our model to construct the near-smooth and impenetrable surface and define the initiator sites (see Supporting Information for details of the concave surface construction). After the cavity (channel) model is constructed, free monomers are filled in the cavity (channel) with reduced number density $\rho_n = 0.85$.

All simulations are performed on NVIDIA Fermi C2050 Graphic Processing Units; for maximum, almost 4 million coarse-grained beads are simulated. With the energy scale ε, the length scale σ_{LJ}, and the bead mass m, the canonical ensemble molecular dynamics simulations are conducted with time step $d_t = 0.002\sigma_{LJ}(m/\varepsilon)^{1/2}$ and $T^* = 1.0k_BT/\varepsilon$. During the simulations of SIP, all data are obtained for the same reaction condition (the polymerization probability $P_r = 0.002$, and the reaction time interval $\tau = 50d_t$, which represents a relatively moderate reaction[23]). Before the polymerization is switched on, a period of 5×10^4 time steps simulation is conducted to eliminate the influence of initial configuration of free monomers. Our simulations include the SIP in spherical cavity with the cavity radius from $7\sigma_{LJ}$ to $95\sigma_{LJ}$, and the SIP in cylindrical channel with channel radius from $7\sigma_{LJ}$ to $115\sigma_{LJ}$. The length of the channel can be arbitrary because we add the periodic boundary condition along the channel axis direction. In practice, we set the length as large as $100\sigma_{LJ}$ so that the finite size effect in simulations can be neglected. The details of each simulated system are listed in the Supporting Information.

In general, there are three scenarios covering all possible experiments measuring PDI for concave SIP. The first scenario is that, for cavities (channels) with various sizes, concave SIPs are carried out for the same period of time (say, 2 h). The second one is also for cavities (channels) with various sizes; concave SIPs are carried out until the same monomer conversion ratio is reached (say, 90%). The third one corresponds to collecting the grown chains with the same average molecular weight for concave SIPs in cavities (channels) with different sizes. It was reported by Kruk et al. that the amount of grafted polymers could be controlled by adjusting the above scenarios, for example, the time of polymerization, in their synthesis of ordered mesoporous carbon.[7] They also observed that, in cases of short polymerization times with specific conditions, the grafted polyacrylonitrile had a relatively low PDI.[27] Therefore, it is indeed essential to verify the PDI and molecular weight dependence on grafting surface curvature for different experimental scenarios in concave SIP.

In accord with these scenarios, we perform three sets of simulations with different grafting surface curvatures and initiator densities but with completely identical polymerization conditions. (The correspondence of grafting density with the initiator density is shown in Supporting Information. With molecular parameters of specific monomers, it is easy to translate reduced grafting density values to the real data, see Supporting Information). In Scenario 1, the polymerization processes are kept for 2000 time units for all the systems. Figure 2a,b shows that, in this set of simulations, the change of PDI with grafting surface curvature is not monotonic. In the region for R^{-1} smaller than 0.028 (R is the radius of cavity or channel, thus, R^{-1} represents the average curvature of the concave surface), PDI increases with enhanced confinement, while in the region $R^{-1} = 0.028-0.14$, PDI surprisingly decreases with increasing surface curvature. In the first region, enhanced confinement surely leads to disparity of growing chains, resulting in an obvious increase of PDI, as suggested previously.[8] However, as the radius of cavity (channels) decreases further, the effective concentration of free monomers near the grafting surface should be much lower than that near flat surface, thus, it indirectly leads to the slowing down of the chain growth, while decelerated polymerization is beneficial to low PDI (see Supporting Information for the observation of slowing down of polymerization). On the other hand, because of the gradual shortage of growing space toward the cavity center (channel axis) as the polymerization proceeds, the enhanced excluded volume interaction significantly depresses

dx.doi.org/10.1021/mz3003374 | ACS Macro Lett. 2012, 1, 1249−1253

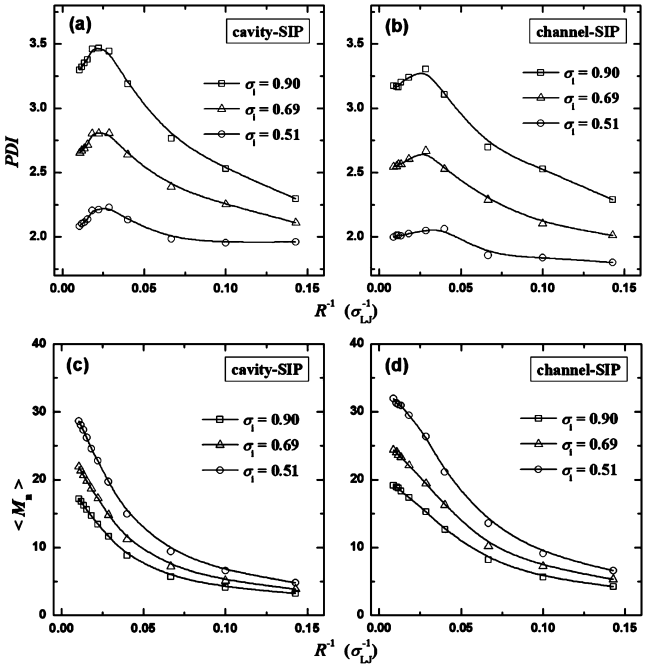

Figure 2. After the same period of polymerization (2000 time units), the PDI dependence on grafting surface curvature with different initiator density (σ_i) in cavity-SIP (a) and in channel-SIP (b) conditions, and the $\langle M_n \rangle$ dependence on grafting surface curvature with different σ_i in cavity-SIP (c) and in channel-SIP (d) conditions.

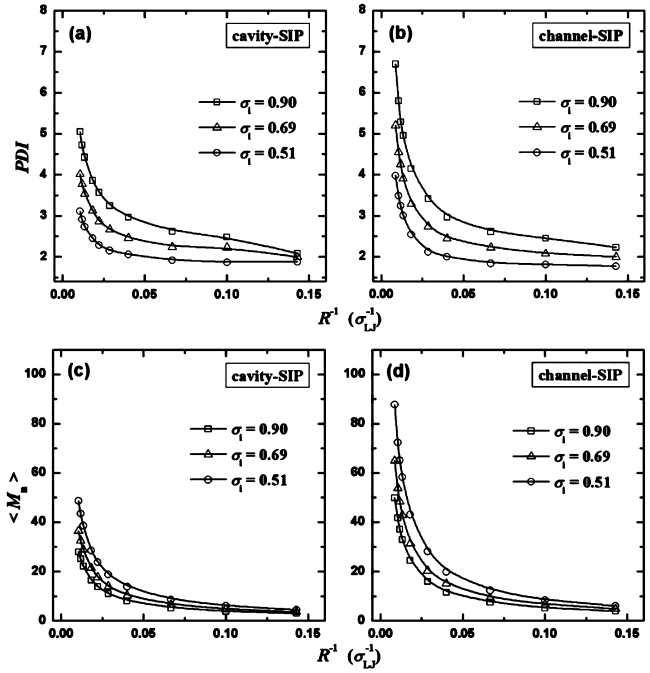

Figure 3. At the same monomer conversion for all the simulations (90%), the PDI dependence on grafting surface curvature with different σ_i in cavity-SIP (a) and in channel-SIP (b) conditions, and the $\langle M_n \rangle$ dependence on grafting surface curvature with different σ_i in cavity-SIP (c) and in channel-SIP (d) conditions.

the chain growth process, which further produces uniformly short growing chains. These unconventional results demonstrate that a critical mesopore size (whose diameter is roughly 70 times larger than the monomer diameter in this study) exists with largest PDI for concave SIP. For example, the molecular diameter of styrene units is 0.593 nm,[28] so we probably obtain the largest PDI for spherical cavity diameter about 41.5 nm. Figure 2 also shows that the PDI values in channel-SIP (Figure 2b) are slightly smaller than those in cavity-SIP (Figure 2a) at the same polymerization condition, as a result of weaker geometric confinement in the cylindrical channel. For further evaluating the overall confinement of the growing chains, we show the dependence of average molecular weight ($\langle M_n \rangle$) on the grafting surface curvature in the first scenario. As shown in Figure 2c,d, $\langle M_n \rangle$ monotonically decreases with increasing surface curvature, implying that enhanced confinement yields the decrease of molecular weight, in agreement with the results of Genzer et al.[8] and Pasetto et al.[21]

Consider the cases that the concave SIP reactions are ceased until all monomers are generally used up. This can be easily fulfilled in experiments by waiting a long enough time during the SIP process. Our second set of simulations (Scenario 2) corresponds to this situation: all the concave SIP reactions are carried out until each system exactly reaches 90% of the monomer conversion. Normally one may imagine that PDI should increase as the surface curvature increases in this situation. But, as shown in Figure 3, the dependence of PDI on grafting surface curvature is completely counterintuitive: PDI actually monotonically decreases with enhanced surface curvature. By analyzing available experimental data, we surprisingly find that some experiments can directly support our result. For example, the experimental results of Pasetto et al.[21] (see the Supporting Information for cited experimental data) showed that, for similar size of particle diameter (375−380 nm), larger mesopore size (0.68 cm^3/g) may yield a higher PDI (6.9) than the smaller pore size (0.23 cm^3/g with PDI = 1.4). Actually, they also indicated that the PDI of grafted PMMA (polymethylmethacrylate) chains increases when both the overall mesopore volume and the ratio between the specific surface and the external surface of the particle are increased, where the increase of mesopore volume exactly corresponds to the decrease of grafting surface curvature. In our results, based on the monotonic change of PDI with surface curvature, we find the larger the cavity (channel) radius, the stronger the influence of surface curvature is. This implies that the influence of surface curvature on PDI is more prominent in the situations with *weaker* confinement. Actually, the cavities (channels) with smaller surface curvature are larger, thus, they can accommodate more monomers. As the reaction proceeds, some short chains may gradually stop growing at the region near to the surface due to the screening of other chains. Therefore, some longer chains with active ends, which are the winners of the growing competition, will consume basically all the monomers left in the cavity (channel) and generate very long chains. This leads to a great disparity of the chain lengths, so a high PDI. Notably in channel-SIP (Figure 3b), the PDI values are generally higher for small surface curvature as compared to cavity-SIP in the same reaction condition. It can be attributed to the fact that in channel-SIP the chains can grow much longer (especially along the channel axis direction) with the same monomer conversion, thus, it is more possible to obtain a broader chain length distribution in this case. One may argue that the experimental PDI values for SIP on flat surfaces (corresponding to grafting surface curvature as zero) are generally very small. But grafting surface curvature approaching zero in our simulations means an extraordinarily large cavity (channel) full of monomers. Therefore, the SIP on a flat surface (in open space) is intrinsically different from the concave SIP

dx.doi.org/10.1021/mz3003374 | ACS Macro Lett. 2012, 1, 1249−1253

condition with curvature approaching zero. Furthermore, from Figure 3c,d, we still find that $\langle M_n \rangle$ monotonically decreases with increasing surface curvature, thus, the conclusion that enhanced confinement yields a decrease of molecular weight is still valid in this scenario.

It should be noted that, for Scenarios 1 and 2, one may suspect the high PDI observed for larger cavities (channels) can be ascribed to polymers being swollen by monomers like that observed in emulsion polymerization. After checking the free monomer density distribution along the cavity (channel) surface normal direction, we find that the density of free monomers in the near-surface region is very low, thus, the high PDI for larger cavities (channels) is not likely due to polymer swollen by free monomers (see Supporting Information for details).

In experiments, we may collect the cleaved chains with the same average molecular weight from cavities (channels) with different sizes. In our third set of simulations, we study the dependence of PDI on grafting surface curvature in cases that the average molecular weights $\langle M_n \rangle$ are basically the same. It should be noted that the unsaturated initiators are also included in the contribution of $\langle M_n \rangle$ with $M_n = 1$. Figure 4 shows that

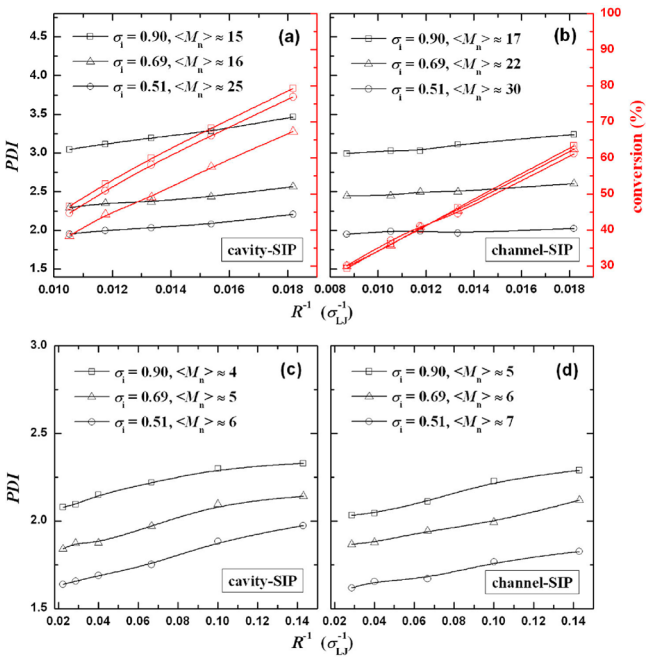

Figure 4. With around the same average molecular weight ($\langle M_n \rangle$) for the same initiator density system, the PDI dependence on grafting surface curvature in cavity-SIP (a) and in channel-SIP (b) conditions with R^{-1} = 0.018−0.14, and the PDI dependence on grafting surface curvature in cavity-SIP (c) and in channel-SIP (d) conditions with R^{-1} = 0.008−0.018. The red lines in (a) and (b) are the corresponding conversions of the systems based on the present PDI values.

the PDI values in systems with relatively larger surface curvature are generally higher. As we know, molecular weight is strongly dependent on grafting surface curvature, thus, in the systems with different grafting surface curvatures, their $\langle M_n \rangle$ values should differ greatly. Therefore, for the sake of clarity, it is appropriate to show the results for the systems with different grafting surface curvatures, that is, for a larger cavity (channel) with R^{-1} = 0.008−0.018 (Figure 4a, b) and for a smaller cavity (channel) with R^{-1} = 0.018−0.14 (Figure 4c,d), respectively. The results in Figure 4 imply that only in this scenario PDI increases with increasing confinement, in harmony with one's intuitive speculation. In Figure 4a,b, we also show the monomer conversions of the systems based on the corresponding PDI values. It is clear that, for the same $\langle M_n \rangle$, the monomer conversions in the systems with larger grafting surface curvatures are higher, indicating that the comparison of PDI in Scenario 3 is not based on the same conversion, in contrast to the cases in Scenario 2. In channel-SIP, the dependence of monomer conversion on grafting surface curvature almost overlaps with each other for different initiator densities. It can be attributed to the weaker confinement in this condition.

We have shown herein that the surface-initiated polymerization is greatly surface curvature dependent. Our results reveal that, depending on different criteria for ceasing the reaction, different relationships between grafted chain PDI and the grafting surface curvature can be categorized. Some previous speculations that the concave SIP seems to lead to a general increase in PDI with increasing surface curvature[8,20,21] may fail to generalize the true dependence of PDI on the surface geometry. Besides, our results also show that the enhanced confinement in concave SIP yields the decrease of molecular weight, which is consistent with experimental results. These results shed light on better control and design of functional porous materials for use in bioimplanting or chemical sensors.

■ ASSOCIATED CONTENT

Supporting Information

Additional information on the model and the methods, as well as supplementary discussion. This material is available free of charge via the Internet at http://pubs.acs.org.

■ AUTHOR INFORMATION

Corresponding Author

*E-mail: luzhy@jlu.edu.cn; zysun@ciac.jl.cn.

Notes

The authors declare no competing financial interest.

■ ACKNOWLEDGMENTS

This work is subsidized by the National Basic Research Program of China (973 Program, 2012CB821500) and supported by the National Science Foundation of China (21025416, 21104025, 20974040) and China Postdoctoral Science Foundation (2012T50286).

■ REFERENCES

(1) Canham, L. T.; Stewart, M. P.; Buriak, J. M.; Reeves, C. L.; Anderson, M.; Squire, E. K.; Allcock, P.; Snow, P. A. *Phys. Status Solidi A* **2000**, *182*, 521.
(2) Zhou, Z.; Zhu, S.; Zhang, D. *J. Mater. Chem.* **2007**, *17*, 2428.
(3) McInnes, S. J. P.; Voelcker, N. H. *Future Med. Chem.* **2009**, *1*, 1051.
(4) Sohn, H.; Létant, S.; Sailor, M. J.; Trogler, W. C. *J. Am. Chem. Soc.* **2000**, *122*, 5399.
(5) Chan, S.; Horner, S. R.; Fauchet, P. M.; Miller, B. L. *J. Am. Chem. Soc.* **2001**, *123*, 11797.
(6) Moreno, J.; Sherrington, D. C. *Chem. Mater.* **2008**, *20*, 4468.
(7) Kruk, M.; Dufour, B.; Celer, E. B.; Kowalewski, T.; Jaroniec, M.; Matyjaszewski, K. *J. Phys. Chem. B* **2005**, *109*, 9216.
(8) Gorman, C. B.; Petrie, R. J.; Genzer, J. *Macromolecules* **2008**, *41*, 4856.
(9) Blas, H.; Save, M.; Boissière, C.; Sanchez, C.; Charleux, B. *Macromolecules* **2011**, *44*, 2577.
(10) Cheng, L.; Cao, D. *ACS Nano* **2011**, *5*, 1102.

(11) Choi, K. Y.; Han, J. J.; He, B.; Lee, S. B. *J. Am. Chem. Soc.* **2008**, *130*, 3920.
(12) Kim, J.-B.; Huang, W.; Bruening, M. L.; Baker, G. L. *Macromolecules* **2002**, *35*, 5410.
(13) Baum, M.; Brittain, W. J. *Macromolecules* **2002**, *35*, 610.
(14) Jones, D. M.; Brown, A. A.; Huck, W. T. S. *Langmuir* **2002**, *18*, 1265.
(15) Prucker, O.; Rühe, J. *Macromolecules* **1998**, *31*, 592.
(16) Marutani, E.; Yamamoto, S.; Ninjbadgar, T.; Tsujii, Y.; Fukuda, T.; Takano, M. *Polymer* **2004**, *45*, 2231.
(17) Turgman-Cohen, S.; Genzer, J. *J. Am. Chem. Soc.* **2011**, *133*, 17567.
(18) Turgman-Cohen, S.; Genzer, J. *Macromolecules* **2012**, *45*, 2128.
(19) Kim, J.-B.; Huang, W.; Miller, M. D.; Baker, G. L.; Bruening, M. L. *J. Polym. Sci., Part A: Polym. Chem.* **2003**, *41*, 386.
(20) Turgman-Cohen, S.; Genzer, J. *Macromolecules* **2010**, *43*, 9567.
(21) Pasetto, P.; Blas, H.; Audouin, F.; Boissière, C.; Sanchez, C.; Save, M.; Charleux, B. *Macromolecules* **2009**, *42*, 5983.
(22) Kruk, M.; Dufour, B.; Celer, E. B.; Kowalewski, T.; Jaroniec, M.; Matyjaszewski, K. *Macromolecules* **2008**, *41*, 8584.
(23) Liu, H.; Li, M.; Lu, Z.-Y.; Zhang, Z.-G.; Sun, C.-C. *Macromolecules* **2009**, *42*, 2863.
(24) Matyjaszewski, K. General Concepts and History of Living Radical Polymerization. In *Handbook of Radical Polymerization*; Matyjaszewski, K., Davis, T. P., Eds.; John Wiley and Sons: New York, 2002; Chapter 8, p 361.
(25) Matyjaszewski, K.; Miller, P. J.; Shukla, N.; Immaraporn, B.; Gelman, A.; Luokala, B. B.; Siclovan, T. M.; Kickelbick, G.; Vallant, T.; Hoffmann, H.; Pakula, T. *Macromolecules* **1999**, *32*, 8716.
(26) Verso, F. L.; Egorov, S. A.; Milchev, A.; Binder, K. *J. Chem. Phys.* **2010**, *133*, 184901.
(27) Kruk, M.; Dufour, B.; Celer, E. B.; Kowalewski, T.; Jaroniec, M.; Matyjaszewski, K. *Polym. Mater. Sci. Eng.* **2007**, *97*, 274.
(28) Marcus, Y. *The Properties of Solvents*; John Wiley and Sons, Ltd.: England, 1999.